units, was stirred with a 0.3 M aqueous solution (4 mL) of KI or KBr and toluene (4 mL) in a 20-mL centrifuge test tube for 3 h at room temperature. The tube was centrifuged at 3000 rpm for 20 min. Aliquots of the aqueous phase were potentiometrically titrated with 0.01 N silver nitrate. Results are reported in Table VI. Values are the average of at least two measurements. The experimental error was within ±5% of the obtained values.

Swelling and Hydration of Catalysts 1a–d. A 0.5-g sample of catalyst was shaken for 3 h at room temperature in a 10-mL graduated centrifuge test tube with 8 mL of toluene, or 8 mL of a 4 M aqueous solution of KI (or KBr), or 4 mL of toluene and 4 mL of a 4 M aqueous solution of potassium salt and then centrifuged for 20 min at 3000 rpm; the catalyst stratified in a compact layer above, below, and at the interface, respectively. The observed swelling volumes of polymers are reported in Table VII. Measurements were reproducible within ±0.1 mL. Samples of centrifuged catalyst were carefully withdrawn, shaken by hand with 1 mL of anhydrous Me_2SO-d_6, filtered, and analyzed by ^1H NMR. The percent of water in the mixture of solvents adsorbed by the catalyst is reported in Table VII. Values are the average of at least two measurements. The experimental error was within ±5%.

Acknowledgment. This paper was supported by a grant from the Progetto Finalizzato di chimica fine e secondaria of Consiglio Nazionale delle Ricerche (CNR), Roma.

Registry No. 4, 88106-63-2; **5**, 81518-75-4; **6**, 88106-65-4; **7**, 76377-04-3; **8**, 88106-64-3; **9**, 16069-36-6; **12**, 14937-45-2; octyl methanesulfonate, 16156-52-8; octyl bromide, 111-83-1.

Kinetic Isotope Effects and Tunneling in Cyclic Double and Triple Proton Transfer between Acetic Acid and Methanol in Tetrahydrofuran Studied by Dynamic ^1H and ^2H NMR Spectroscopy

Detlef Gerritzen and Hans-Heinrich Limbach*

Contribution from the Institut für Physikalische Chemie der Universität Freiburg i.Br., D-7800 Freiburg, West Germany. *Received December 28, 1982*

Abstract: We have extended our previous studies of proton exchange and hydrogen bonding between acetic acid (A) and methanol (B) in tetrahydrofuran-d_8 to the study of the primary kinetic H/D isotope effects of the exchange. For this purpose a new combination of dynamic ^1H and ^2H NMR spectroscopy has been used to perform an "NMR proton inventory". The following rate law was obtained at deuterium fractions $D = 0$ and $D = 1$ of the exchangeable protonic sites: $v = k^{LL}C_AC_B + k^{LLL}C_A{}^2C_B$ (L = H, D). This was attributed to a superposition of cyclic double and triple proton exchange involving one and two molecules of acetic acid and one molecule of methanol. Additional experiments were carried out at intermediate deuterium fractions. Thus, we have succeeded in measuring the kinetic HH/HD/DD and HHH/HHD/DDD isotope effects of the exchange as a function of the temperature. This has been achieved for the first time for well-defined intermolecular multiple-proton-transfer reactions. We discuss the possibility of determining the number of protons transferred in a chemical reaction by performing an NMR proton inventory. The rule of the geometric mean (RGM) is fulfilled for the kinetic isotope effects of the LLL process, which are almost independent of temperature within the margin of error. By contrast, the RGM is not fulfilled for the LL process, and the kinetic isotope effects depend strongly on the temperature. The energies of activation and frequency factors fit Bell's criteria of tunneling. Our kinetic results are not in good agreement with predictions of transition-state theory but can be explained by an intermolecular tunneling model. The results are proof that acetic acid and methanol form cyclic hydrogen-bonded 1:1 and 2:1 complexes which have a very low concentration in tetrahydrofuran.

Noncatalyzed proton-transfer reactions (HH reactions) of the type

$$AH + XH^* = BH^* + XH \quad (1)$$

can take place between a variety of molecules in protic and aprotic[1-20] media and in the gaseous and the solid[21-24] state. In organic and biochemical systems they are related to bifunctional catalysis[25-33] and biological activity.[34-36] On the other hand, these

(1) Bell, R. P. "The Tunnel Effect in Chemistry"; Chapman and Hall: London, 1980.
(2) Grunwald, E. In "Proton Transfer"; Caldin, E., Gold, V., Eds.; Chapman and Hall: London, 1975; p 103.
(3) Denisov, G. S.; Bureiko, S. F.; Golubev, N. S.; Tokhadze, K. G. In "Molecular Interactions"; Ratajczak, H., Orville-Thomas, W. J., Eds.; Wiley: Chichester, 1980; Vol. 2, p 107.
(4) Limbach, H. H. In "Aggregation Processes in Solution"; Gormally, J., Wyn Jones, E., Eds.; Elsevier: Amsterdam, 1983; Studies in Physical and Theoretical Chemistry, Vol. 26, Chapter 16, p 411.
(5) Limbach, H. H.; Seiffert, W. *Ber. Bunsenges. Phys. Chem.* **1974**, *78*, 641.
(6) Limbach, H. H. *Ber. Bunsenges. Phys. Chem.* **1977**, *81*, 1112.
(7) Limbach, H. H. *J. Magn. Reson.* **1979**, *36*, 287.
(8) Hennig, J.; Limbach, H. H. *J. Chem. Soc., Faraday Trans. 2* 1979, 75, 752.
(9) Limbach, H. H.; Hennig, J. *J. Chem. Phys.* **1979**, *71*, 3120.
(10) Limbach, H. H.; Seiffert, W. *J. Am. Chem. Soc.* **1980**, *102*, 538.
(11) Gerritzen, D.; Limbach, H. H. *J. Phys. Chem.* **1980**, *84*, 799.
(12) Limbach, H. H.; Gerritzen, D.; Seiffert, W. *Bull. Magn. Reson.* **1980**, *2*, 315.
(13) Gerritzen, D.; Limbach, H. H. *Ber. Bunsenges. Phys. Chem.* **1981**, *85*, 527.
(14) Limbach, H. H.; Hennig, J.; Gerritzen, D.; Rumpel, H. *Faraday Discuss. Chem. Soc.* **1982**, *74*, 229.
(15) Hennig, J.; Limbach, H. H. *J. Magn. Reson.* **1982**, *49*, 322.
(16) Limbach, H. H.; Hennig, J.; Stulz, J. *J. Chem. Phys.* **1983**, *78*, 5432.
(17) Bureiko, S. F.; Denisov, G. S.; Golubev, N. S.; Lange, I. Y. *React. Kinet. Catal. Lett.* **1979**, *11*, 35.
(18) Bren, V. A., Chernoivanov, V. A.; Konstantinovskii, L. E.; Nivorozhkin, L. E.; Zhdanov, Y. A.; Minkin, V. I. *Dokl. Akad. Nauk SSSR* **1980**, *251*, 1129.
(19) Nesmeyanov, A. N.; Babin, V. N.; Zavelovitch, E. B.; Kochetkova, N. S. *Chem. Phys. Lett.* **1976**, *37*, 184.
(20) Graf, F. *Chem. Phys. Lett.* **1979**, *62*, 291.
(21) Schuster, P., Zundel, G., Sandorfy, C., Eds.; "The Hydrogen Bond"; North-Holland Publishing Co.: Amsterdam, 1976.
(22) Nagoka, S.; Terao, T.; Imashiro, F.; Saika, A.; Hirota, N.; Hayashi, S. *Chem. Phys. Lett.* **1981**, *80*, 580.
(23) Meier, B. H.; Graf, F.; Ernst, R. R. *J. Chem. Phys.* **1982**, *76*, 767.
(24) Baugham, S. L.; Duerst, R. W.; Rowe, W. F.; Smith, Z.; Wilson, E. B. *J. Am. Chem. Soc.* **1981**, *103*, 6286.
(25) Swain, C. G.; Brown, J. F. *J. Am. Chem. Soc.* **1952**, *74*, 2534, 2538.

0002-7863/84/1506-0869$01.50/0

Scheme I

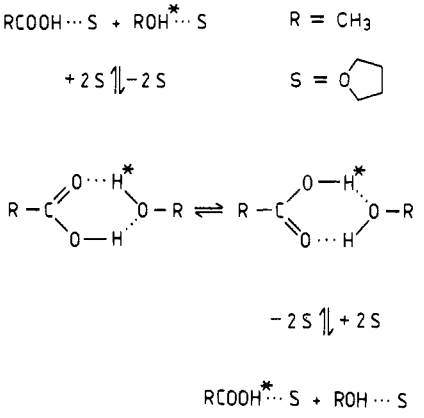

Scheme II

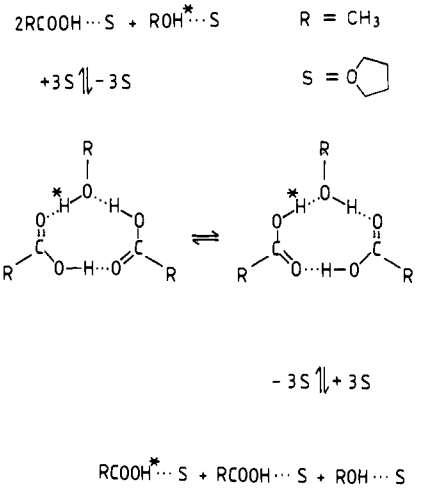

reactions are an old topic of theoretical chemistry.[9,21,37-44] In solution, tunneling probabilities should be higher in the case of neutral HH transfer than in an ionic single-H-transfer reaction because there is no need for the solvent molecules to reorientate[1,45] around the reacting molecules. The participation of tunneling in proton-transfer reactions can be verified by a measurement of the primary kinetic isotope effects (KIE).[1] The study of the full KIE, e.g., the HH/HD/DH/DD KIE in LL reactions, where L = H or D, is, therefore, necessary for the elucidation of the reaction mechanisms.

It has been known for a long time[46-49] that for reactions in aqueous solution more than one proton donor can contribute to the observed KIE either because of a different H/D composition in the proton donor site with respect to the solvent (fractionation) or because a number of $n > 1$ of protons is transported in the rate-limiting step. In order to deduce n from the kinetic data the "rule of the geometric mean"[50] (RGM) has been extensively used in the subsequent "fractionation factor theory". For $n = 2$ this rule specifies the following relation between the bimolecular rate constants:

$$k^{HD} = (k^{HH}k^{DD})^{1/2} \quad (2)$$

Little is known, however, of the validity of this assumption. It can be verified only by studying the KIE of proton-transfer reactions where n is known a priori, i.e., without using the RGM. Though the kinetics of several HH reactions[4-13,15-20] have been studied in the past by dynamic NMR spectroscopy, only very recently[14] have we reported, in continuation of our previous work,[4-13,15,16] full HH/HD/DD KIE for well-defined double-proton-transfer reactions. The data were reported[14] for the intermolecular LL migration in *meso*-tetraphenylporphine (TPP), in part also for azophenine (AP), and in a preliminary form for proton exchange in the system acetic acid/methanol/tetrahydrofuran (THF). The KIE were compared with the predictions of transition-state theory and different tunneling theories. The KIE of TPP could be explained by a vibrational model of tunneling in a fixed symmetrical double-minimum potential with discrete NH stretching levels.[14,16]

In this paper we report the KIE of proton exchange between acetic acid and methanol in THF, which we obtained by performing a "proton inventory"[35,36,46-49] where reaction rates are measured as a function of the deuterium fraction D of the exchangeable protonic sites. These experiments have been realized for the first time by a combination of dynamic ^1H and ^2H NMR spectroscopy. Grunwald et al.[2] had found evidence for nonionic proton transfer between carboxylic acids and alcohols as a side reaction of ionic exchange in protic media. Although ionic proton transfer can, in principle, be important in aprotic media,[3,4,7,10,17] we have shown that the NMR line shapes of very pure acetic acid/methanol/THF samples are affected only by cyclic, nonionic proton exchange,[6,7,10] which we discussed in terms of a 1:1 proton exchange between the reactants (Scheme I). In addition to this double proton transfer we find now by extending the reactant concentration range a second cyclic process in which two acetic acid molecules and one methanol molecule participate, i.e., a triple proton transfer (Scheme II). We report here the HH/HD/DD and HHH/HHD/DDD KIE for the two reactions. We found that the RGM is obeyed only in the triple-proton-transfer process. It will be shown that this behavior and the values found for the frequency factors and the energies of activation cannot be explained by transition-state theory but can be explained easily by an intermolecular tunneling model.[14]

Experimental Section

Sample Preparation. Methanol, acetic acid, and THF were purchased from Merck (Darmstadt) and their deuterated analogues from Fluka

(26) Cox, M. M.; Jencks, W. P. *J. Am. Chem. Soc.* **1981**, *103*, 580.
(27) Bell, R. P.; Critchlow, J. E. *Proc. R. Soc. London, Ser. A* **1971**, *325*, 35.
(28) Ek, M.; Ahlberg, P. *Chem. Scr.* **1980**, *16*, 62.
(29) Engdahl, K. A.; Bivehed, H.; Ahlberg, P.; Saunders W. H., Jr. *J. Chem. Soc., Chem. Commun.*, **1982**, 423.
(30) Klaer, A. M.; Nielsen, H.; Sorenson, P. E.; Ulstrup, J. *Acta Chem. Scand., Ser. A* **1980**, *A34*, 281.
(31) Bensaude, O.; Dreyfus, M.; Dodin, G.; Dubois, J. E. *J. Am. Chem. Soc.* **1977**, *99*, 4438.
(32) Bensaude, O.; Chevrier, M.; Dubois, J. E. *J. Am. Chem. Soc.* **1979**, *101*, 2423.
(33) Albery, W. J. *J. Chem. Soc., Faraday Trans. 1* **1982**, *78*, 1579.
(34) Albery, W. J. *Faraday Discuss. Chem. Soc.* **1982**, *74*, 245.
(35) Gandour, R. D.; Schowen, R. L. "Transition States of Biochemical Processes"; Plenum Press: New York, 1978.
(36) Elrod, J. P.; Gandour, R. D.; Hogg, J. L.; Kise, M.; Maggiora, G. M.; Schowen, R. L.; Venkatasubban, K. S. *Symp. Faraday Soc.* **1975**, *10*, 145.
(37) Lowdin, P. O. *Rev. Mod. Phys.* **1963**, *35*, 22.
(38) Ady, E.; Brickmann, J. *Chem. Phys. Lett.* **1971**, *11*, 302.
(39) Graf, F.; Meyer, R.; Ha, T. K.; Ernst, R. R. *J. Chem. Phys.* **1981**, *75*, 2914.
(40) Brickmann, J.; Zimmermann, H. *Ber. Bunsenges. Phys. Chem.* **1966**, *70*, 157, 521; **1967**, *71*, 160.
(41) German, E. D.; Kusnetzov, A. M.; Dogonadze, R. R. *J. Chem. Soc., Faraday Trans. 2* **1980**, *76*, 1128 and references cited herein.
(42) Bruniche-Olsen, N.; Ulstrup, J. *J. Chem. Soc., Faraday Trans. 1* **1979**, *75*, 205.
(43) Kusnetzov, A. M.; Ulstrup, J. *J. Chem. Soc., Faraday Trans. 2* **1982**, *78*, 1497.
(44) de la Vega, J. R. *Acc. Chem. Res.* **1982**, *15*, 185.
(45) Caldin, E. F.; Mateo, S. *J. Chem. Soc., Faraday Trans. 2* **1975**, *71*, 1876.
(46) Gross, P.; Steiner, H.; Krauss, F. *Trans. Faraday Soc.* **1936**, *32*, 877. Hornell, J. C.; Butler, J. A. V. *J. Chem. Soc.* **1936**, 1361.
(47) Gold, V. *Trans. Faraday Soc.* **1960**, *56*, 255. Gold, V. *Adv. Phys. Org. Chem.* **1969**, *7*, 259.
(48) Kresge, A. J. *Pure Appl. Chem.* **1964**, *8*, 243.
(49) Albery, W. J. In ref 2, Chapter 9, p 263.
(50) Bigeleisen, J. *J. Chem. Phys.* **1955**, *23*, 2264.

(Ulm), Merck (Darmstadt), and ICN (Munich). A vacuum glass apparatus described previously[11] was used for the preparation of sealed NMR samples of known composition and high purity, both crucial to this work. Only greaseless Teflon needle valve stopcocks were employed. The purified and degassed solvents, stored in glass vessels over a drying agent, were transferred partly into graduated capillary tubes by successive evaporation and condensation. This procedure allowed volume measurements at any desired temperature, though generally at room temperature, before condensation into the NMR tube was effected. In the last stage the NMR tube was sealed off. THF was dried over sodium/potassium alloy with anthracene as drying indicator. A special effort was necessary to dry methanol and acetic acid over molecular sieve (Merck, 3 Å), and the following procedure had to be employed. Molecular sieve was placed in a glass vessel and activated in vacuo at 360 °C with an electric oven. Without separating the vessel from the vacuum line, methanol or acetic acid was then condensed from a second vessel on the molecular sieve. In the case of CL_3COOD and CL_3OD the molecular sieve was deuterated with D_2O before the activation. For the acceleration of the drying process the liquids were refluxed by cooling the upper parts of the vessels with liquid nitrogen. The next day the methanol or acetic acid was condensed into the second glass vessel, the molecular sieve was activated again, and the liquid was recondensed on the molecular sieve. This procedure was carried out four times. In this way CH_3OH, CH_3OD, CD_3OH, CD_3OD, CH_3COOH, CH_3COOD, CD_3COOH, CD_3COOD, and certain CL_3OH/CL_3OD and CL_3COOH/CL_3COOD mixtures were prepared. The molecular sieve used for drying the mixtures was first treated with H_2O/D_2O with a deuterium fraction corresponding to the value desired for the exchangeable protonic sites in the mixtures. The capillary tube system with the NMR tube sealed to it was then attached to the vacuum line. The NMR tube contained a H_2O/D_2O mixture with the desired deuterium fraction. After evaporation dry THF was condensed into the tube and then back into the storage vessel in order to remove traces of water from the inner glass walls. This procedure was repeated twice. Dry methanol and acetic acid were condensed into the capillary tubes to deuterate the walls and then evaporated into the cooling traps of the vacuum line. Then the NMR samples were prepared as described above. Although this procedure demands much effort, it has the advantage that samples can be prepared with desired and defined deuterium fractions and reactant concentrations. We estimate concentration errors of less than 5%, i.e., below the NMR detection limit, for, in calculating the NMR line shapes, we never found evidence for concentrations other than those calculated from the volume measurements in vacuo.

Care also had to be taken in choosing an optimal sample size. In order to minimize concentration errors we used NMR tubes with an outer diameter of 8 mm (Wilmad, Buena, inner tube no. 516 i). The volume of the liquid phase in the samples was then about 2 mL. The gas-phase volume was kept by appropriate sealing to a value of about 0.5–1 mL. The total length of the NMR samples was about 5 cm. For the NMR measurements the 8-mm NMR samples were placed in an outer 10-mm NMR tube (Wilmad, no. 516 o). By limiting the gas-phase volume we obtained a homogeneous sample temperature, which is especially important above room temperature. When the volume of the gas phase extended to the spinner turbine, which was at room temperature, refluxing of the liquid could not be avoided. This refluxing was accompanied by dramatic differences in the relative reactant concentrations between the liquid and the gas phase.

^{1}H and ^{2}H NMR Spectroscopic Measurements. The ^{1}H and ^{2}H NMR spectra were measured with a pulse FT NMR spectrometer, Bruker CXP 100, working at 90.02 MHz for protons and at 13.816 MHz for deuterons. The spectrometer was equipped with a 10-mm probe for both nuclei. For the ^{1}H NMR experiments the internal lock device was employed and for the ^{2}H NMR experiments an external ^{19}F lock. All spectra were obtained without sample spinning in order to obtain line profiles which are not affected by spinning side bands. The sample temperatures were monitored with a set of thermometers calibrated against the chemical shift of CH_3OH according to Van Geet.[51] In general, simple phase alternating pulse sequences were used. Longitudinal relaxation times were measured with the inversion–recovery method.[52] The spectra were transferred from the Bruker Aspect 2000 minicomputer to a Commstore II floppy disk (Sykes) equipped with a RS 232 interface and then to the Univac 1108 computer of the Rechenzentrum der Universität Freiburg, via a direct data line. The kinetic data were obtained by simulation of the experimental spectra using a computer program based on the quantum-mechanical density-matrix formalism described previously[7] for intermolecular spin exchange between high-order spin systems. In the spectra presented here, the coupling constants J_{CHOD} and J_{CDOD} were so small that the OH or the OD site of methanol could be treated as a one-spin system. The line shapes depended on the proton (deuteron) lifetime τ_{AL} in acetic acid (A), the lifetime τ_{BL} in methanol (B), the chemical shifts of the exchangeable protons (deuterons) in A and B, and the effective transverse relaxation times T_2^{eff}. The lifetimes are interrelated by

$$\tau_{AL}/\tau_{BL} = C_{AL}/C_{BL} \qquad L = H,D \tag{3}$$

where

$$C_{AH} + C_{AD} = C_A \tag{4}$$

C_A and C_B are the total concentrations of A and B known from the sample preparation. The individual deuterium fractions, given by

$$D_A = C_{AD}/C_A \tag{5}$$

differ from the known overall deuterium fraction

$$D = (C_{AD} + C_{BD} + ...)/(C_A + C_B + ...) \tag{6}$$

when the equilibrium constant K_f of the fractionation reaction

$$AH + BD = AD + BH \tag{7}$$

is not unity. K_f can be written in the form

$$K_f = \frac{C_A(D + \tau_{BH}/\tau_{AH}) + C_B(D-1)}{C_B(D + \tau_{AH}/\tau_{BH}) + C_A(D-1)} = \frac{C_B(1 + \tau_{AD}/\tau_{BD}) - D(C_A + C_B)}{C_A(1 + \tau_{BD}/\tau_{AD}) - D(C_A + C_B)} \tag{8}$$

and can, thus, also be obtained from the line-shape simulations.

The T_{2eff} are given for the case of extreme motional narrowing by the equation[53]

$$\pi W_0 = T_{2eff}^{-1} = T_1^{-1} + \pi W_{inhom} \tag{9}$$

where W_0 is the line width in the absence of exchange and W_{inhom} is the contribution of the magnetic field inhomogeneity. The ^{1}H T_1 values were found to be on the order of seconds so that W_0 was given only by W_{inhom} in the case of the ^{1}H NMR experiments. W_{inhom} was obtained by measuring the ^{1}H NMR line width of tetramethylsilane dissolved in THF-d_8. By contrast, the ^{2}H T_1 values could not be neglected in eq 7. They were obtained from a sample of 0.2 M CH_3COOD and from a sample of 0.2 M CH_3OD in THF as a function of the temperature. We used the following expression obtained from the literature[54]

$$T_1^{-1} = x_A/T_{1A} + x_B/T_{1B} \tag{10}$$

where x_i are the mole fractions of reactant i and $x_A + x_B = 1$. The validity of eq 10 was checked experimentally in some of the ternary mixtures. The T_1 values did not depend on the concentration within the margin of error. W_{inhom} was determined from a sample of acetone-d_6 in THF, which had quite long T_1 values. W_{inhom} was on the order of 2–6 Hz for both the ^{1}H and the ^{2}H measurements. This procedure to determine T_{2eff} is of sufficient accuracy as long as no value of $\tau_{AL}^{-1} < 10$ s^{-1} is extracted from the spectra. We did not attempt to obtain accurate values below this limit by using, for example, magnetization-transfer methods.[15] The ^{1}H chemical shifts of the system $CH_3COOH/CH_3OH/THF$-d_8 were determined in a previous study[11] and may be written for 90 MHz in the form

$$\nu_A = 1103.9 - 0.537T + 57.42C_A \exp(-548.5/T) + 13.72C_B \exp(-129.9/T) \tag{11a}$$

$$\nu_B = 434.0 - 0.5698T + 9.298C_A \exp(-312.7/T) + 6.937C_B \exp(344.0/T) \tag{11b}$$

From eq 11a and 11b we took the quantity $\Delta\nu = \nu_A - \nu_B$ needed in the NMR line-shape calculations of the RCOOH/ROH signals above the coalescence point. Below this point ν_A and ν_B were determined by simulation, and the validity of eq 11 was checked. The ^{2}H NMR spectra were treated in a similar way. A fairly constant value of $\Delta\nu = 102 \pm 1$ Hz was found at low temperatures for the different samples, which is in good agreement with eq 11 after account is taken of the different Larmor frequency of ^{2}H. Figure 1 shows the superposition of experimental and calculated ^{1}H NMR line shapes of the system $CD_3COOH/CD_3OH/THF$-d_8 as a function of the temperature. The lines are very broad because of the coalescence of the COOH and the OH signals. The strong sharp signal arising from the residual CH pro-

(51) Van Geet, A. L. *Anal. Chem.* **1970**, *42*, 679.
(52) Farrar, T. C.; Becker, E. "Pulse and Fourier Transform NMR"; Academic Press: New York, 1971.
(53) Abragem, A. "The Principles of Nuclear Magnetism"; Clarendon Press: Oxford, 1961.
(54) Strehlow, H.; Frahm, J. *Ber. Bunsenges. Phys. Chem.* **1975**, *79*, 57.

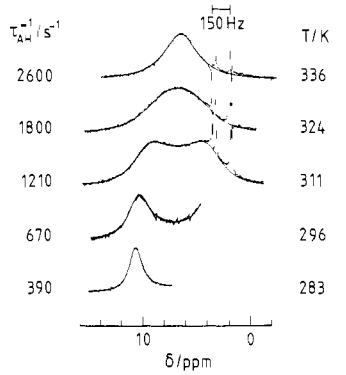

Figure 1. Superposed experimental and calculated ^1H 90.02-MHz FT NMR difference spectra of a solution of 0.4 mol L^{-1} CD_3COOH and 0.4 mol L^{-1} CD_3OH in THF-d_8 and of pure THF-d_8 at different temperatures using a 10-mm probe head (1000 scans, 60 pulses, 10-s repetition time, nonspinning sample). The sealed sample tube had a diameter of 8 mm and a height of 40 mm and was placed in a 10-mm NMR tube. The gas phase in the sample was about 20% of the total sample volume. The small sharp peaks arise from the residual aliphatic protons of the solvent and the solutes.

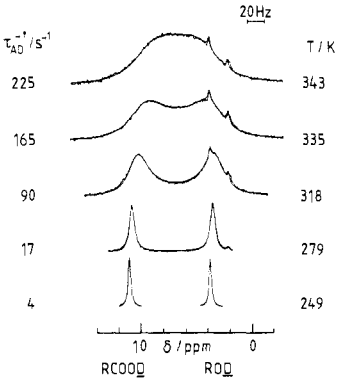

Figure 2. Superposed experimental and calculated ^2H 13.82-MHz FT NMR spectra of a solution of 0.29 mol L^{-1} CH_3COOD and 0.29 mol L^{-1} CH_3OD in THF at different temperatures using the same same sample design as in Figure 1 (500–1000 scans, 60 pulses, 4-s repetition time, nonspinning sample). The deuterium fraction of the exchangeable protons was $D = 0.99$. The small two sharp lines arise from the natural deuterium content of THF. The size of the sample was as in Figure 1.

tons of the solvent (about 1%) made it necessary to subtract the spectra from a reference THF-d_8 sample of similar size. In our previous CW NMR study[10] we were not able to obtain such spectra. Figure 2 shows the superposed experimental and calculated ^2H NMR spectra of a sample of $CH_3COOD/CH_3OC/THF$. The natural-abundance solvent deuterons appear as sharp singlets. The good signal-to-noise ratio and the very large exchange-broadened NMR spectra together with the optimized sample preparation technique provide accurate kinetic data.

The NMR Proton Inventory

In the case of proton-transfer reactions the kinetic information contained in the ^1H NMR line shape is especially high when the exchanging protons are part of high-order spin systems.[7] In favorable cases the number n of protons that participate in the exchange process can be obtained.[7,10] Spin–spin splittings involving deuterons are, however, much smaller, and kinetic isotope effects cannot be obtained in this way. A more general method is to perform a "proton inventory",[33-36,46-49] in which rate constants are measured as a function of the total deuterium fraction D of the exchangeable protons in the samples. In contrast to usual kinetic experiments where overall rate constants are measured, it is possible to obtain individual ^1H and ^2H rate constants by a combination of ^1H and ^2H NMR spectroscopy. Since we report here the first example of such an "NMR proton inventory plot", we discuss in this section the information one can get by using this method.

Single Intermolecular Proton Transfer. We consider the reaction

$$AH + B = A + BH \quad (12)$$

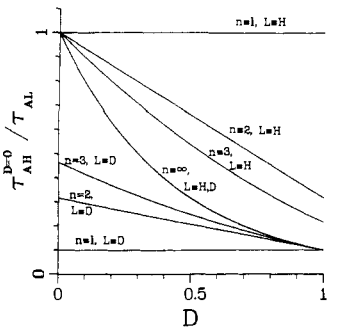

Figure 3. NMR proton inventory plots as a function of the deuterium fraction D for different numbers n of protons transported in the rate-limiting step for C_B = constant. L is the nucleus whose NMR spectra are observed. $\tau_{AD}(D = 1)/\tau_{AH}(D = 0)$ was set arbitrarily to a value of 10.

The quantities measured by ^1H and ^2H NMR are the inverse proton and deuteron lifetimes (eq 3)

$$\tau_{AH}^{-1} = v_{AH}/c_{AH} = k^H C_B \quad (13)$$

$$\tau_{AD}^{-1} = v_{AD}/C_{AD} = k^D C_B \quad (14)$$

where $v = v_{AH} + v_{AD}$ is the overall reaction rate. τ_{AH} and τ_{AD} do not depend on the deuterium fractions, as shown in Figure 3.

Double Intermolecular Proton Transfer. We consider the reaction

$$AH^* + BH = AH + BH^* \quad (15)$$

The NMR lifetimes are given by

$$\tau_{AH}^{-1} = v_{AH}/C_{AH} = ((1 - D_B)k^{HH} + D_B k^{HD})C_B \quad (16)$$

$$\tau_{AD}^{-1} = v_{AD}/C_{AD} = ((1 - D_B)k^{DH} + D_B k^{DD})C_B \quad (17)$$

$$\tau_{BH}^{-1} = v_{BH}/C_{BH} = ((1 - D_A)k^{HH} + D_A k^{HD})C_A \quad (18)$$

$$\tau_{BD}^{-1} = v_{BD}/C_{BD} = ((1 - D_A)k^{DH} + D_A k^{DD})C_A \quad (19)$$

Of special importance are the values of $\tau_{AH}(D = 1)$ measured by ^1H NMR and of $\tau_{AD}(D = 0)$ measured independently by ^2H NMR. The following relation must hold when C_B = constant:

$$\tau_{AH}(D = 1)/\tau_{AD}(D = 0) = k^{HD}/k^{DH} = K_f \quad (20)$$

If the equilibrium constant K_f of the fractionation reaction eq 7 is close to unity, then the observation—as shown in Figure 3—that

$$\tau_{AH}(D = 1) = \tau_{AD}(D = 0) \quad (21)$$

for C_B = constant is the best proof for a double-proton-transfer reaction. Actually, in Figure 3 we, arbitrarily, assumed absence of fractionation and applied the RGM (eq 2); i.e., $k^{HD} = k^{DH} = (k^{HH}k^{DD})^{1/2}$. k^{HH}/k^{DD} was set to a value of 10.

Triple Intermolecular Proton Transfer. We consider the reaction

$$AH^* + BH' + XH = AH + BH^* + XH' \quad (22)$$

We obtain

$$\tau_{AH}^{-1} = ((1 - D_B)(1 - D_X)k^{HHH} + (1 - D_B)D_X k^{HHD} + D_B(1 - D_X)k^{HDH} + D_B D_X k^{HDD})C_B C_X \quad (23)$$

$$\tau_{AD}^{-1} = ((1 - D_B)(1 - D_X)k^{DHH} + (1 - D_B)D_X k^{DHD} + D_B(1 - D_X)k^{DDH} + D_B D_X k^{DDD})C_B C_X \quad (24)$$

k^{HHH} and k^{HDD} are obtained from $\tau_{AH}(D = 0)$ and $\tau_{AH}(D = 1)$, k^{DHH} and k^{DDD} from $\tau_{AD}(D = 0)$ and $\tau_{AD}(D = 1)$, and the other mixed rate constants from a measurement of τ_{BL} and τ_{XL}. For the construction of the curves for $n = 3$ in Figure 3 we assumed again absence of fractionation; i.e.

$$k^{HHD} = k^{HDH} = k^{DHH} \text{ etc.} \quad (25)$$

Additionally, the RGM was arbitrarily applied again. It is interesting to note that, as shown in Figure 3, the proton-transfer

rate τ_{AH}^{-1} is smaller at $D = 1$ than the deuteron-transfer rate τ_{AD}^{-1} at $D = 0$; this is because k^{HDD} is smaller than k^{DHH}.

Superposed Intermolecular Double and Triple Proton Transfer. For the description of the proton exchange in the system acetic acid/methanol/THF we set A = X = CL_3COOL, add eq 16 and 23 as well as eq 17 and 24, and, using eq 25, obtain in the absence of fractionation for the pseudo-second-order rate constants

$$(\tau_{AH}C_B)^{-1} = (1 - D)k^{HH} + Dk^{HD} + C_A((1 - D)^2k^{HHH} + 2(1 - D)Dk^{HHD} + D^2k^{HDD}) = a^H + b^HC_A \quad (26)$$

$$(\tau_{AD}C_B)^{-1} = (1 - D)k^{DH} + Dk^{DD} + C_A((1 - D)^2k^{DHH} + 2(1 - D)Dk^{DDH} + D^2k^{DDD}) = a^D + b^DC_A \quad (27)$$

At a given value of D the pseudo-second-order rate constants are a linear function of C_A. We will interpret our experimental results with these equations, which describe curves that lie somewhere between the curves $n = 2$ and $n = 3$ in Figure 3, depending on the value of C_A. Although in eq 26 and 27 absence of fractionation was assumed, from which it follows that $k^{HD} = k^{DH}$ and $k^{HHD} = k^{HDH} = k^{DHH}$, etc., we still keep the different notations because we want to indicate the method used for the determination of the rate constant. The first superscript H or D in k^{LL} and k^{LLL} indicates then whether the constant has been derived by ^1H or ^2H NMR.

Multiple Intermolecular Proton Transfer. Although we employed the RGM in constructing the illustrative curves of Figure 3, so far we have not actually used the RGM in deriving the equations given above. If n becomes greater than 3 the experimental data generally do not contain enough information in order to decide whether the RGM is fulfilled or not. If one assumes the validity of the RGM, which implies that all single KIE are equal and given for constant total concentrations C_i by

$$\phi^{-1} = (\tau_{AD}(D = 1)/\tau_{AH}(D = 0))^{1/n} \quad (28)$$

one obtains

$$\tau_{AH}^{-1} = \tau_{AH}^{-1}(D = 0)(1 - D + D\phi)^{n-1} \quad (29)$$

$$\tau_{AD}^{-1} = \tau_{AH}^{-1}(D = 0)\phi(1 - D + D\phi)^{n-1} \quad (30)$$

These equations can be easily verified for the case $n = 3$ by some simple transformations of eq 23 and 24 using eq 28. Equations 29 and 30 hold for all values of n. A consequence of the validity of the RGM is that

$$\tau_{AH}/\tau_{AD} = \phi = \text{constant} \quad (31)$$

over the whole range of D. Formally, eq 29 and 30 resemble the Gross–Butler equation,[35,46-49] with the difference that eq 29 and 30 have the exponent $n - 1$ instead of n and that two independent equations can be measured instead of one. Therefore, eq 29 and 30 contain more information than the Gross–Butler equation. The number of protons n involved in the reaction can be easily obtained with eq 28 and 31 by measuring the quantities $\tau_{AH}(D = 0)$, $\tau_{AD}(D = 1)$, and two values of τ_{AH} and τ_{AD} at the same deuterium fraction, e.g., at $D = 0.5$. When the number of protons transferred becomes effectively infinite, as may be the case in pure protic solvents such as methanol, where the exchange may take place by autoprotolysis,[13] and when the overall KIE ϕ^{-n} is finite, ϕ must be close to one and the lifetimes τ_{AH} and τ_{AD} measured by ^1H and ^2H NMR become equal, as shown in Figure 3.

Intramolecular Proton Transfer. We use the term intramolecular proton transfer if the proton-exchanging complex is the dominant species and if this complex is stable on the NMR time scale, i.e., when the proton-transfer rate is faster than the dissociation rate of the complex. A protonated complex then remains protonated and a deuterated complex deuterated on the NMR time scale. In favorable cases, the two can be distinguished in the NMR spectrum. Changing the deuterium fraction changes only the relative NMR intensities of the different isotopic species, as we have observed, for example, in the case of TPP-H_2, TPP-HD, and TPP-D_2[14,16] for an intramolecular double proton transfer. The rate constants k^{HH}, k^{HD}, and k^{DD} are derived directly from the signals of the different isotopic species, and there is no continuous D-dependent rate function as in the intermolecular case. However, for the limits $D = 0$ and $D = 1$, the predictions for the intra- and the intermolecular case coincide. E.g., from ^1H NMR one obtains in the limit $D = 1$ the values of k^H, k^{HD}, or k^{HDD} etc. for a single-, double-, and triple-proton-transfer reaction, and from ^2H NMR, k^D, k^{DH}, and k^{DHH}, in the limit $D = 0$.

Table I. Longitudinal Relaxation Times T_1 of the Exchangeable Deuterons at 13.82 MHz for the THF Solutions

0.2 mol L^{-1} CH_3COOD		0.2 mol L^{-1} CH_3OD	
T/K	T_1/s	T/K	T_1/s
256	0.170 ± 0.006	256	0.245 ± 0.001
265	0.186 ± 0.003	264	0.275 ± 0.005
276	0.208 ± 0.003	276	0.352 ± 0.005
281	0.234 ± 0.001	281	0.406 ± 0.002
299	0.267 ± 0.003	299	0.501 ± 0.003
310	0.322 ± 0.005	309	0.587 ± 0.014
317	0.338 ± 0.002	323	0.719 ± 0.008
323	0.306 ± 0.007	335	0.799 ± 0.008
341	0.446 ± 0.004	340	0.809 ± 0.009

Results

A total of 115 proton lifetimes were obtained from 16 samples of the system $CD_3COOL/CD_3OL/THF\text{-}d_8$, and 165 deuteron lifetimes were obtained from 16 $CH_3COOL/CH_3OL/THF$ samples as a function of the concentrations, deuterium fraction, and the temperature. The data are available as supplementary material. We found by simulation of the NMR line shapes that

$$\tau_{BL} = \tau_{AL}C_{BL}/C_{AL} \approx \tau_{AL}C_B/C_A$$

was fulfilled within the margin of error, where C_B/C_A was known from the sample preparation. Therefore, only τ_{AL} was varied in the line-shape calculations. This observation means that within the margin of error no fractionation of H and D between acetic acid and methanol was observed; i.e., the fractionation constants K_f were unity. We do, however, not exclude a fractionation constant of the order of 0.96 as found by Gold and Lowe[55] for fractionation between acetic acid and water. Table I contains the longitudinal relaxation times of the exchangeable deuterons in the systems CH_3COOD/THF and CH_3OD/THF which were needed for the line-shape simulations as mentioned earlier. Because of the difficulty of NMR studies of a series of samples at exactly the same temperature, we employed the following procedure for determining the rate law of the proton exchange. For each sample the experimental pseudo-first-order rate constants τ_{AL}^{-1} were fitted to the Arrhenius law by varying the preexponential factor and the energy of activation. Using these parameters, we then calculated for each sample the pseudo-second-order rate constants τ_{AL}^{-1}/C_B at given temperatures. These constant did not depend on the methanol concentration, which indicates that only one methanol molecule participates in the exchange process. This result is consistent with our previous[7,10] ^1H NMR line-shape studies of the system $CH_3COOH/CH_3OH/THF\text{-}d_8$. The pseudo-second-order rate constants were, however, a linear function of the acetic acid concentration C_A as shown for 298 K in Figure 4. Thus, the exchange could be described by the superposition of a LL reaction involving one molecule of each methanol and acetic acid and an LLL reaction involving two acetic acid molecules and one methanol molecule. In our previous CW ^1H NMR study[10] we did not detect the HHH reaction because large line widths could not be measured for experimental reasons and C_A was kept small. In this study we carried out concentration-dependent ^1H NMR experiments at $D = 0$ and $D = 0.8$ and ^2H NMR experiments at $D = 0.2$ and $D = 0.99$ and obtained for each temperature four curves as shown in Figure 4 from which the rate constants and activation parameters given in Table II were derived as follows. Since the curves were linear in C_A they could

(55) Gold, V.; Lowe, B. M. *J. Chem. Soc. A* **1968**, 1936.

Table II. Kinetic Parameters of Proton Exchange in the System Acetic Acid/Methanol/Tetrahydrofuran[a]

T/K	k^{HH}	k^{HD}	k^{DH}	k^{DD}	k^{HHH}	k^{DHH}	k^{DDD}
255	112 ± 23				400 ± 87		
260	144 ± 30				528 ± 114		
265	184 ± 40				691 ± 150		
270	232 ± 50				895 ± 195		
275	291 ± 66				1146 ± 254		
280	362 ± 84		58 ± 4	16 ± 11	1459 ± 327	678 ± 16	135 ± 31
285	446 ± 108		76 ± 5	22 ± 13	1838 ± 420	861 ± 17	167 ± 37
290	547 ± 137	93 ± 23	97 ± 6	30 ± 15	2299 ± 536	1085 ± 21	206 ± 44
295	666 ± 173	124 ± 32	124 ± 8	41 ± 17	2852 ± 690	1357 ± 31	250 ± 52
298	746 ± 198	147 ± 38	143 ± 11	48 ± 19	3235 ± 782	1547 ± 40	281 ± 57
300	805 ± 217	164 ± 43	156 ± 13	54 ± 20	3514 ± 857	1685 ± 48	303 ± 60
305	967 ± 270	213 ± 58	196 ± 20	70 ± 23	4300 ± 1073	2078 ± 73	364 ± 70
310	1156 ± 334	274 ± 75	243 ± 29	91 ± 26	5227 ± 1334	2546 ± 107	434 ± 80
315	1374 ± 411	349 ± 98	301 ± 41	117 ± 30	6316 ± 1648	3099 ± 153	515 ± 91
320	1624 ± 503	440 ± 125	369 ± 57	148 ± 34	7586 ± 2025	3750 ± 213	607 ± 104
325	1910 ± 611		450 ± 76	186 ± 38	9062 ± 2472	4511 ± 289	711 ± 117
330	2235 ± 738		545 ± 101	231 ± 43	10766 ± 3000	5399 ± 385	828 ± 132
335	2604 ± 887		656 ± 132	286 ± 48	12728 ± 3622	6427 ± 505	960 ± 150
E_a	28.0 ± 1	34.8 ± 2		40.8 ± 2	30.7 ± 2	31.9 ± 2	27.7 ± 3
$\log A$	7.8 ± 0.2	8.3 ± 0.2		8.8 ± 0.2	8.9 ± 0.2	8.8 ± 0.1	7.3 ± 0.2

$(k^{HH}/k^{DD})_{298K} = 15.5 \pm 4.4$
$(k^{HH}/k^{HD})_{298K} = 5.1 \pm 1.4$
$(k^{HD}/k^{DD})_{298K} = 3.1 \pm 0.9$
$(k^{HH}/k^{DD})_{280K} = 6.1 \pm 1.5$
$(k^{HH}/k^{HD})_{280K} = 4.0 \pm 1.0$

$(k^{HHH}/k^{DDD})_{298K} = 11.5 \pm 2.7$
$(k^{HHH}/k^{HHD})_{298K} = 2.1 \pm 0.5$

[a] k^{HH} and k^{HHH} were determined by using eq 26 at $D = 0$ by ^{1}H NMR. k^{DD} and k^{DDD} were determined at $D = 0.99$ by using eq 27 by ^{2}H NMR. The k^{HD} were determined by using eq 32 at $D = 0.8$ by ^{1}H NMR, and k^{DH} and k^{DHH} were determined by using eq 33 and 34 at $D = 0.2$ by ^{2}H NMR. The k^{LL} are given in L mol^{-1} s^{-1} and the k^{LLL} in L mol^{-2} s^{-2}, where L = H or D. The energies of activation are given in kJ mol^{-1}. A = frequency factor. The error limits given for k^{LL} and k^{LLL} were obtained by linear least-squares fitting. Since the statistical errors of E_a and A were found to be unacceptably small, the error limits listed here for these quantities were estimated.

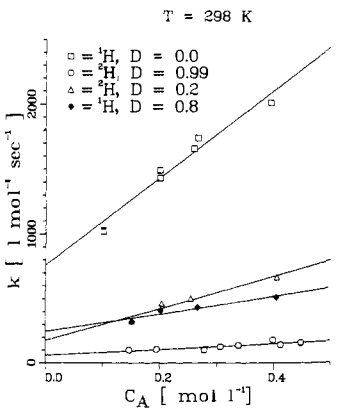

Figure 4. Pseudo-second-order rate constants of proton exchange in the system acetic acid (A) and methanol (B) at 298 K as a function of the total concentration C_A of acetic acid and the deuterium fraction D. (□) and (♦) were obtained by ^{1}H and (△) and (○) by ^{2}H NMR spectroscopy.

be described by eq 26 and 27. From these equations it follows that k^{HH} and k^{DD} are the intercepts of the curves ^{1}H,$D = 0$ and ^{2}H,$D = 0.99$ in Figure 4. The intercepts of the two middle curves in Figure 4 are given by

$$a(^1\text{H},D = 0.8) = 0.8k^{HD} + 0.2k^{HH} \quad (32)$$

$$a(^2\text{H},D = 0.2) = 0.8k^{DH} + 0.2k^{DD} \quad (33)$$

from which we calculate independent values for k^{HD} and k^{DH} given in Table II. They coincide within error limits: as eq 21 emphasizes, this is proof for the existence of double proton transfer. It is especially impressive in view of the fact that two totally independent methods were employed. The k^{HHH} and k^{DDD} values listed in Table II were given by the slopes of the ^{1}H,$D = 0$ and ^{2}H,$D = 0.99$ curves shown for 298 K in Figure 4. For the two middle curves the slopes are given according to eq 26 and 27 by

$$b(^2\text{H},D = 0.2) = 0.64k^{DHH} + 0.32k^{DDH} + 0.04k^{DDD} \quad (34)$$

$$b(^1\text{H},D = 0.8) = 0.04k^{HHH} + 0.32k^{HHD} + 0.64k^{HDD} \quad (35)$$

For the evaluation of k^{DHH}, we set first the right side of eq 34 equal to k^{DHH}. This approximation results in a value of k^{DHH} that is only about 20% too small. In this way, we obtained a KIE of $k^{HHH}/k^{DHH} = 2.2$ at 298 K, which was in good agreement with the RGM value (eq 2) of $\phi^{-1} = (k^{HHH}/k^{DDD})^{1/3} = 2.26$. The same agreement was found also for other temperatures. Therefore, we knew now that the RGM is fulfilled for the LLL process within the margin of error. So we calculated the refined k^{DHH} values listed in Table II using eq 34 by setting $k^{DHH}/k^{DDH} = k^{DDH}/k^{DDD} = \phi^{-1}$. This correction reduced, however, k^{HHH}/k^{DHH} only very slightly to a value of 2.1. The error of k^{DHH} is given by the error of the slope $b(^2\text{H},D = 0.2)$ because the k^{DHH} term is the most important term in eq 34. The situation is, however, less favorable for the determination of the k^{HDD} because the three terms in eq 35 are of comparable magnitude in view of the fact that $k^{HHH} > k^{DHH} > k^{HDD}$. In other words, the error of the calculated k^{HDD} values depends not only on the error of $b(^1\text{H},D = 0.8)$ but also on the error of k^{HHH} and k^{DHH}. Therefore, we were not able to determine k^{HDD} from the ^{1}H NMR measurements at $D = 0.8$. Since the RGM is, however, fulfilled for the LLL process, we calculated k^{HHD} when necessary from k^{DDD}. This suggests that, in the future, ^{1}H NMR experiments in particular should be performed at deuterium fractions much higher than 0.8, where the proton exchange rates will no longer be affected by k^{HHH} and k^{HHD}. The choice of lower deuterium fractions in the ^{2}H NMR experiments is less important because k^{DDH} and k^{DDD} are smaller than k^{DHH}. In a final stage of evaluation of the data, we recalculated the theoretical Arrhenius curves for each sample, i.e., the pseudo-first-order rate constants. Since the LL and the LLL reaction contribute to these constants, the corresponding Arrhenius curves are expected to be nonlinear. The deviation of the calculated curves from linearity was, however, small and could, therefore, not be detected experimentally. Thus, our procedure for evaluating the kinetic data is consistent.

In addition to the experiments described above, we performed a ^{1}H and ^{2}H proton inventory at 298 K and a concentration of $C_A = C_B = 0.2$ mol L^{-1}. Some of the ^{2}H NMR spectra are shown in Figure 5. The increase in the exchange broadening clearly indicates that the deuteron lifetimes are shortened by lowering the deuterium fraction. The experimental lifetimes are available

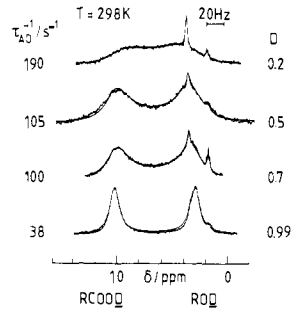

Figure 5. Superposed experimental and calculated ^2H 13.82-MHz FT NMR spectra of solutions of 0.3 mol L^{-1} CH_3COOL and 0.3 mol L^{-1} CH_3OL (L = H, D) in THF at 298 K as a function of the deuterium fraction D (500–5000 scans, 60 pulses, 4-s repetition time, nonspinning sample). The sample design was as in Figure 1.

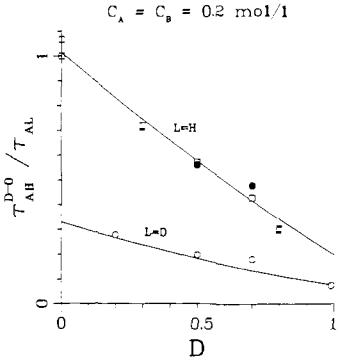

Figure 6. Experimental NMR proton inventory plot at 298 K and a concentration of 0.2 mol L^{-1} for the two reactants: (□) data obtained by ^1H NMR of the system $CD_3COOL/CD_3OL/THF$-d_8; (■) data obtained by ^1H NMR of the system $CH_3COOL/CH_3OL/THF$ (selective pulses on the COOH signal); (○), data obtained by ^2H NMR of the system $CH_3COOL/CH_3OL/THF$. The curves were calculated according to eq 26 and 27 by using the rate constants listed in Table II and a value of $k^{HDD} = 634$ L mol^{-2} s^{-2} calculated from k^{DDD} using the RGM.

as supplementary material and are plotted in Figure 6 as open circles together with the curves calculated with eq 26 and 27 and the known values of k^{LL} and k^{LLL}. We obtain good agreement between the calculated curves and the experimental data. For a pure $n = 2$ process the value of the upper curve at $D = 1$ and the lower curve at $D = 0$ should be equal. Since at $C_A = 0.2$ mol L^{-1} the $n = 3$ process contributes to the exchange, the experimental curves lie between the theoretical $n = 2$ and $n = 3$ curves. It is interesting to calculate the mean number n of protons transferred from the data in Figure 6 by using eq 29 and 30. From sample 9 and 22, where $D = 0.5$, we obtained $\tau_{AH}^{-1}(D = 0.5) = 160$ s^{-1} and τ_{AD}^{-1} $(D = 0.5) = 55$ s^{-1}, which gives $\phi^{-1} = 2.91$. With $\tau_{AH}^{-1}(D = 0) = 290$ s^{-1} (sample 2) and τ_{AD}^{-1} $(D = 0.99) = 20$ s^{-1} (sample 27) we obtained with eq 28 a mean value of $n = 2.5$ at 298 K and $C_A = C_B = 0.2$ mol L^{-1}. This result was obtained in an early stage of the experiments and helped us to recognize the presence of the $n = 3$ process.

We wanted further to confirm that the KIE did not depend within the margin of error on the H/D substitution in the aliphatic CL sites of the reactants and of the solvent corresponding to secondary substrate and solvent KIE. For this purpose we measured some proton lifetimes by using selective excitation of the COOH signals (90° pulses, duration 5 ms) of the $CH_3COOL/CH_3OL/THF$ samples no. 22–25 for which we had already obtained the deuteron lifetimes by ^2H NMR (Table III). The last values are represented for samples no. 22 and 25 in the lower curve of Figure 6 at $D = 0.5$ and 0.7 by open circles. The proton lifetime of these two samples are represented in Figure 6 by filled circles. They lie nicely on the calculated line derived from the data of the $CD_3COOL/CD_3OL/THF$-d_8 samples. We obtained a similar agreement also for samples no. 23 and 24 as shown in Table III. In any of these samples the proton lifetime is much smaller than the deuteron lifetime. These results mean

Table III. Pseudo-Second-Order Rate Constants $(\tau_{AH}C_B)^{-1}$ Obtained from the Line-Shape Analysis of the COOH Signal in the System $CH_3COOL(A)/CH_3OL(B)/THF$ Measured at 90.02 MHz and 298 K[a]

SN	$(\tau_{AH}C_B)_{exptl}^{-1}$/ (L mol^{-1} s^{-1})	$(\tau_{AH}C_B)_{calcd}^{-1}$/ (L mol^{-1} s^{-1})	C_A/ (mol L^{-1})	C_B/ (mol L^{-1})	D
22	772	800	0.205	0.203	0.5
23	877	975	0.205	0.203	0.5
24	578	700	0.302	0.304	0.7
25	660	580	0.204	0.202	0.7

[a] Selective pulses were used in order to suppress the high-field signals. The calculated values were obtained by using eq 24 and the rate constants listed in Table II. For k^{HDD} a value of 643 mol L^{-2} s^{-2} was adopted calculated from k^{DDD} by using the RGM. SN is the sample number which refers to those in Appendices I and II of the Supplementary Material. C_A and C_B are the concentrations of acetic acid and methanol, and D is the deuterium fraction.

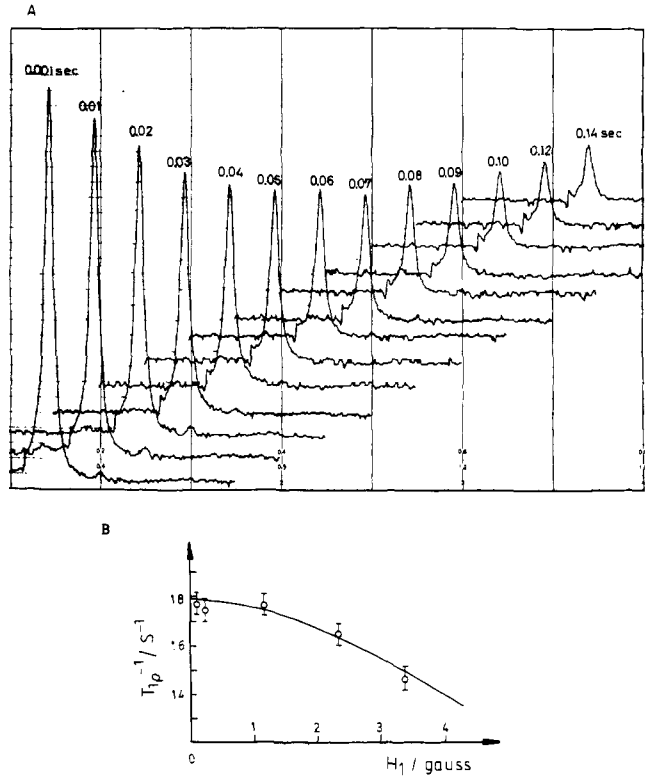

Figure 7. ^1H 90.02-MHz NMR $T_{1\rho}$ experiment on the coalesced COOH/OH line at 7.3 ppm of a mixture of 0.08 mol L^{-1} CH_3COOH and 0.08 mol L^{-1} CH_3OH in methylcyclohexane-d_{14} at 298 K: (a) line intensity as a function of the spin locking pulse length (100 scans, B_1 = 1 G, 30-s repetition time, spinning sample); (b) $1/T_1$ as a function of the spin locking pulse strength B_1. Using the experimental value of $T_1 = 6.2$ s we obtained $\Delta\nu = 594 \pm 20$ Hz and $\tau_{AH}^{-1} = 8.8 \times 10^4$ s^{-1}, which corresponds to a pseudo-second-order proton-exchange rate constant of 10^6 L mol^{-1} s^{-1}.

that we cannot detect a secondary KIE in this system with our present margin of error. This error is especially large for the selective-excitation experiments, where the aliphatic signals are still very strong (even though they have been reduced in intensity by a factor of about $^1/_{30}$). It is clear that this method only works in a region where the COOH signal is not too greatly broadened by exchange, because of its overlap with the aliphatic proton signals.

In order to obtain an idea of how the use of an inert solvent influences the proton-exchange rates, we prepared a sample of 0.08 M CH_3COOH and 0.08 M CH_3OH in methylcyclohexane-d_{14} (MCY). Proton exchange is much faster in this sample than in a similar THF sample, and a coalesced COOH/OH line with an exchange broadening of about 6 Hz is found at 298 K

in the ^1H 90.02-MHz FT NMR spectrum. We performed selective $T_{1\rho}$ experiments in the rotating frame on the coalesced line, as shown in Figure 7a. We used the same experimental setup as described previously.[8,15] Figure 7b shows the dependence of $T_{1\rho}^{-1}$ on the strength of the magnetic field B_1 of the spin locking pulse. From this dependence, the proton lifetime τ_{AH} and the chemical shift difference $\Delta\nu$ were obtained according to the equation[51]

$$T_{1\rho}^{-1} = T_1^{-1} + \tfrac{1}{2}\pi^2\Delta\nu^2\tau_{AH}(1 + \gamma^2B_1^2\tau_{AH}^2/4)^{-1} \quad (36)$$

where γ is the gyromagnetic ratio. We obtain a value of $\Delta\nu$ = 594 Hz, which is similar to the values found for THF-d_8 (eq 11), and a value of $\tau_{AH}^{-1} = 8.8 \times 10^4$ s^{-1}, which gives a pseudo-second-order rate constant of 1.1×10^6 L mol s^{-1}. This corresponds to a kinetic MCY/THF solvent effect of about 10^3.

Discussion

Kinetic Solvent Effects. We interpret our results in terms of a superposed double and triple proton exchange in cyclic hydrogen-bonded complexes as shown in Schemes I and II. Proof of these mechanisms is the lack of methanol self-exchange[10] and the experimental rate law eq 26 and 27. For the cyclic HH process we have obtained an additional very important proof by finding that eq 21 is fulfilled for low concentrations of acetic acid. As shown previously,[10,11] the reactants are predominantly hydrogen bonded to the solvent S. By measuring the chemical shifts in this system, we showed that small percentages of linear complexes RCOOH···RCOOH···S, RCOOH···ROH···S, ROH···RCOOH···S, and ROH···ROH···S are present. The cyclic complexes of Schemes I and II are present in so low a concentration that they do not affect the chemical shifts. These cyclic complexes are detected only by the kinetic experiments. Since we cannot observe different lines for the different hydrogen-bonded environments, the case of fast hydrogen-bond formation and dissociation is realized on the NMR time scale although the proton transfer is slow and rate determining. Therefore, the observed rate constants are the product of an exchange rate constant k_{ex} within the cyclic complex and an equilibrium constant K_c of the formation of the cyclic complex from the reactants[10]

$$k = k_{ex}K_c = k_{ex}\exp(-\Delta H/RT + \Delta S/R) \quad (37)$$

ΔH is the difference in enthalpy and ΔS in entropy between the solvent hydrogen-bonded reactants and the cyclic complexes. As we have shown previously,[10,11] ΔS can be written in the form

$$\Delta S = \Delta S_0 - nR \ln C_S \quad (38)$$

where C_S is the concentration of the solvent which acts as a hydrogen-bond acceptor and n the number of solvent molecules liberated during the formation of the cyclic process, i.e., $n = 2$ for the LL and $n = 3$ for the LLL process (Schemes I and II). ΔS_0 is the entropy of the complex formation for standard state of unit solvent concentration. Because of the great value of C_S the association equilibria are shifted to the side of the quasi-monomeric species, which lowers the rate constants of the exchange. In the inert solvent methylcyclohexane no such hydrogen bonds are formed with the solvent and the exchange is, in consequence, faster. However, self-association of the reactants can also impede the formation of the less stable cyclic complexes, which should also result in a contribution to the lowering of the proton-exchange rates at lower temperatures and higher reactant concentrations. The k^{HH} values derived in this study for the system $CD_3COOH/CD_3OH/THF$-d_8 are slightly smaller than the values we reported previously[10] for the system $CH_3COOH/CH_3OH/THF$-d_8. This is not a secondary KIE but the consequence of the fact that we had not previously recognized the presence of the HHH process. This affects the pseudo-second-order rate constants. However, within the margin of error, the energy of activation and the preexponential factor of the HH process listed in Table II are identical with those derived previously.[10] Hence, our previous interpretations of these quantities are still valid. From the high frequency factor of the HH process, we concluded[10] that no solvated ion pair (lower pathway in Scheme III) is formed as intermediate. The solvent molecules would be oriented around such an ion pair $A^-H_2B^-$, leading to a considerable loss in entropy. For such a mechanism one should, therefore, have found a much more negative entropy of activation.[10]

Scheme III

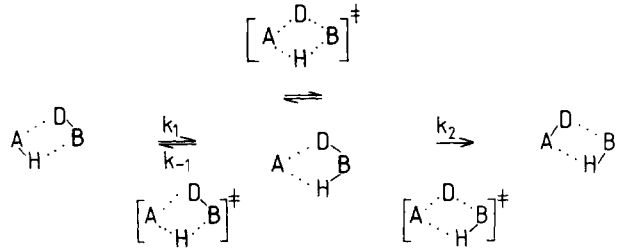

Kinetic Isotope Effects in Transition-State Theory. Moreover, we can exclude this solvated ion pair mechanism by discussing the KIE in terms of transition-state theory (TST). The ionic reaction pathway of Scheme III involves two transition states between the ionic intermediate and the reactants. These TS's are degenerate in the case of the HH and the DD reaction but nondegenerate in the HD reaction because of the different zero-point energies (ZPE) of the remaining BH and BD stretching vibrations. For the particularly simple case where the vibration of the nontransferred H or D remains the same in the intermediate and in the first TS (i.e., when secondary KIE are neglected), we have derived the equation[14]

$$k^{HD}/k^{DD} = 2/(1 + k^{DD}/k^{HH}) \quad (39)$$

for the case of a symmetrical double-proton-transfer reaction. The RGM would, therefore, not be fulfilled, and at low temperatures, where $k^{DD}/k^{HH} \ll 1$, it follows that $k^{HD}/k^{DD} = 2$; i.e., the energies of activation of the HD and the DD processes would become equal. This is in contradiction to the experimental results given in Table II for our HH process. In fact, at 280 K we find a value of $k^{HD}/k^{DD} = 4$, which is twice as great as the value predicted by eq 39. Thus the KIE, the high frequency factors, and the different values of E_a^{HD} and E_a^{DD} all offer evidence against a solvated ion pair as intermediate. As we have previously shown,[14] TST predicts that the RGM should be fulfilled to a good approximation if the reaction proceeds in a synchronous way via the symmetrical TS as indicated in the upper pathway of Scheme III. The KIE should then result from different energies of activation and the relation

$$E_a^{HD} = (E_a^{HH} + E_a^{DD})/2 \quad (40)$$

should be fulfilled. This is easily shown by inserting the Arrhenius law into eq 2 and setting all frequency factors equal.

$E_a^{DD} - E_a^{HH}$ can have a maximum value of about 10 kJ mol^{-1}, which corresponds to the loss of the ZPE of two stretching vibrations in the TS, with one frequency imaginary and the other close to zero. The k^{HH}/k^{DD} value should then be the square of the maximum single H/D KIE, i.e., on the order of 40–70 at room temperatures. We find, however, for the LLL process that the KIE of 12.5 at 298 K arises mainly from the fact that $A^{HHH} > A^{DDD}$. The margin of error in the E_a^{LLL} does not allow us to make with precision the statement that all E_a^{LLL} are equal (it even seems that E_a^{DDD} is smaller than E_a^{HHH}). *However, there is no experimental doubt that the temperature-dependent contribution to the KIE is significantly smaller than the temperature-independent contribution.* Generally, this behavior cannot be explained by TST. However, Koch and Dahlberg[56] have shown that A^D may be significantly smaller than A^H if the dissociation rate constant of the proton-transfer complex is comparable to the proton-transfer rate within the complex. This interpretation seems, however, unlikely in the cases discussed here because—as mentioned above—the rates of interconversion between the hydrogen-bonded complexes are very fast on the NMR time scale in contrast to the proton-transfer rates. However, we cannot completely exclude

(56) Koch, H. F.; Dahlberg, D. B. *J. Am. Chem. Soc.* **1980**, *102*, 6102.

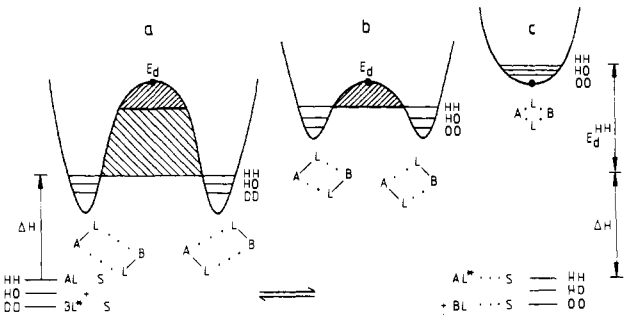

Figure 8. Tunneling model for an intermolecular HH migration. For further explanation see text.

such an interpretation in the case of the LLL process because we do not know the ratio between dissociation and proton-transfer rate constants.

By contrast, the KIE in the LL reaction are caused by a difference in the energies of activation, $E_a^{DD} - E_a^{HH} = 13$ kJ mol^{-1}, which is higher than predicted by TST. The large HH/DD KIE of 15.5 at 298 K is a consequence of this high value. The KIE would be even higher if A^{HH} were not 10 times smaller than A^{DD}. Thus, in the LL process, the Bell criteria of tunneling[1] are fulfilled.

Tunneling Model. We discuss our results in terms of a tunneling model[14] which unifies the Bell model of tunneling,[1] tunneling in a double-well potential,[40] and transition-state theory of proton transfer with a proton-stable transition state as shown in Figure 8. One essential feature of the model is that it takes into account cyclic complex formation; i.e., the rate constants are described by eq 37. Tunneling cannot occur outside this complex. In the low-temperature regime, k_{ex} may become independent of temperature and then may be identified with a ground-state tunneling rate k_{t0}. For this case (as readily seen from eq 37) there is still a dependence of the exchange rate constant k on the temperature: the energy of activation is now given by the enthalpy ΔH of complex formation. In other words, a minimum energy, corresponding to that required to assemble the reactants into the proper structure, is required for tunneling to occur. In principle, there might be an equilibrium isotope effect on complex formation from the reactants, but such an effect should be relatively small and we will neglect it. The consequence is that in this regime, as depicted in Figure 8a, the KIE become independent of temperature because they are determined only by the KIE on k_{ex} (which is equal to k_{t0} at low temperatures). Assuming a parabolic barrier, k_{t0} can be written in one-dimensional WKB approximation[1] in the form[1,9,14,40]

$$k_{t0} = \nu(l/\pi^{l-1})P_0 \qquad l = 1, 2 \tag{41}$$

$$P_0 = \exp[-(2^{3/2}\pi^2/h)(E_d - E_0)Q(l)/E_d^{1/2}] \tag{42}$$

$$Q(l) = \xi_0 m^{1/2}/l \tag{43}$$

ν is the frequency with which the particle strikes the barrier, m the tunneling mass, and ξ_0 the barrier half-width. In the energy-splitting model (ES model), where $l = 2$, the tunnel rates are related to the resonance tunnel splittings of states in a double-minimum potential.[9,14,40] This resonance tunnel effect is not taken into account in the transmission (TR) method, where $l = 1$. In principle, the tunneling mass is not constant as the reaction proceeds and depends on whether the protons move in a synchronous or in an asynchronous manner. Using the one-dimensional approximation we have evaluated the quantity Q by means of a mass-weighted coordinate system for the synchronous and the asynchronous pathway[9,14]

$$2Q_{syn} = (\sum_{i=1}^{N} \Delta r_i^2 m_i)^{1/2}/l \tag{44}$$

$$2Q_{asyn} = \sum_{i=1}^{N} \Delta r_i m_i^{1/2}/l \tag{45}$$

N is the number of atoms that are displaced during the reaction and Δr_i is the distance over which the ith atom is transported when the reaction coordinate ξ changes from $-\xi_0$ to $+\xi_0$. We are aware that neither a completely synchronous nor asynchronous pathway is realized in practice. However, as we have discussed previously[9,14] and as can be seen immediately by substituting eq 44 and 45 into eq 42, the tunneling probability is much higher along the synchronous than along the asynchronous pathway. This is because, to a good approximation,

$$Q_{asyn} = N^{1/2}Q_{syn} \tag{46}$$

The summation in eq 44 and 45 must be extended over all atoms, e.g., also over the oxygen atoms of acetic acid, which slightly change position. We will, however, neglect this intramolecular heavy-atom motion. If only H or D move and if they all move along the same distance Δr, it is useful to introduce the mass-dependent quantity

$$Q' = Q/(\sum m_i)^{1/2} = \Delta r(N^{1/2})^{1-s}/2l \tag{47}$$

Q' is one of the four parameters that describe one set of Arrhenius curves. For an asynchronous pathway $s = 0$ and for a synchronous pathway $s = 1$.

In intermolecular exchange such as that under study here, we have to take into account that the distance R_{AB} in the hydrogen-bonded complex is flexible; the consequence of this flexibility if broad AL stretching bands in the IR spectra of hydrogen-bonded systems.[21,57] There is, therefore, a distribution of intermolecular vibrational states within the complex, which corresponds to a distribution of mean distances R_{AB} between the heavy atoms of the reacting molecules AH and BH, as shown in Figure 8b,c. Indeed, Eliason and Kreevoy[58] have taken into account just such a distribution of double-minimum potentials for proton transfer in their paper on the KIE for hydrolytic reactions. In free solution, it would be correct to use a continuum of intermolecular states.[21] The barrier height E_d for proton transfer between AH and BH decreases as R_{AB} decreases, i.e., as intermolecular excited states are populated (Figure 8b,c). At high energies, i.e., very short R_{AB}, there is no longer any barrier to the proton transfer. This behavior of hydrogen-bonded systems has been known, at least in principle, for a long time.[21,57-59] However, we have no experimental knowledge of the dependence $E_d = E_d(R_{AB})$ and are, therefore, obliged to set E_d = constant as shown in Figure 8. We will use the term *soft double-minimum potential* for a continuous distribution of different double-minimum potentials in contrast to a single, *tight double-minimum potential*, such as is required to describe the hydrogen migration in porphines.

For the different isotopic reactions, we may introduce different barrier heights

$$E_d^{DD} = E_d^{HH} + \Delta\epsilon = E_d^{HD} + \Delta\epsilon/2 \tag{48}$$

where $\Delta\epsilon$ contains all changes in zero-point energies (ZPE) by going from the reactants to the proton-stable transition state (TS) shown in Figure 8b. We do not exclude a small barrier along the potential curve of Figure 8c which might be of the order of the ZPE. The existence of a proton-stable TS, where the imaginary frequency is associated with a heavy-atom motion, has been discussed in the literature[35,58] although actual proton-transfer reactions have been, generally, explained in terms of a proton-unstable TS, where an AH stretching vibration becomes imaginary. Albery and Limbach[60] have discussed the question of how the force constants have to be chosen in order to produce a proton-stable or a proton-unstable TS. As shown in Figure 8c, a cyclic complex AH_2B as TS may contain an appreciable amount of ZPE so that $\Delta\epsilon$ may be small. As in the early work of Doganadze et

(57) Novak, A., *Struct. Bonding (Berlin)* **1974**, *14*, 177.
(58) Eliason, R.; Kreevoy, M. M. *J. Am. Chem. Soc.* **1978**, *100*, 7037.
(59) Gunnarson, G.; Wennerstrom, H.; Egan, W.; Forsen, S. *Chem. Phys. Lett.* **1976**, *38*, 96. Altman, L. J.; Laungani, D.; Gunnarsson, G.; Wennerstrom, H.; Forsen, S. *J. Am. Chem. Soc.* **1978**, *100*, 8264.
(60) Albery, W. J.; Limbach, H. H. *Faraday Discuss. Chem. Soc.* **1982**, *74*, 291.

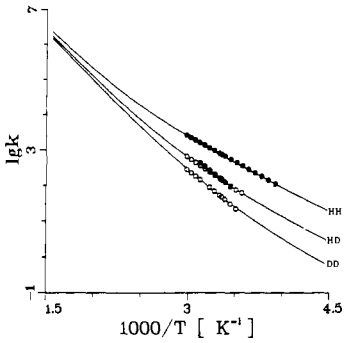

Figure 9. Arrhenius curves of the intermolecular double HH, HD, and DD exchange involving one molecule each of acetic acid and methanol in tetrahydrofuran. The three curves were calculated according to the tunnel model in Figure 7 using only four parameters given in Table III: (●) values obtained by ^{1}H NMR spectrocopy; (○) values obtained by ^{2}H NMR spectroscopy.

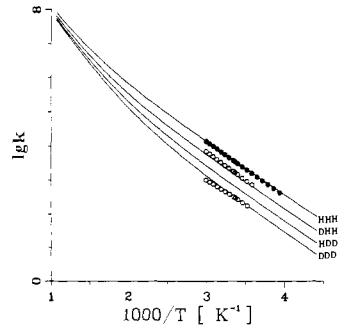

Figure 10. Arrhenius curves of the intermolecular triple HHH, HHD, HDD, and DDD exchange involving one molecule and two molecules of acetic acid in tetrahydrofuran. The four curves were calculated according to the tunnel model in Figure 7 using only four parameters given in Table III: (●) values obtained by ^{1}H NMR spectroscopy; (○) values obtained by ^{2}H NMR spectroscopy.

al.[41,42] we consider here only tunneling between the vibrational ground states on both sides of the barrier; i.e., at higher energies the reaction takes place at shorter R_{AB}. Using a continuous Boltzmann distribution for the intermolecular states we obtain from eq 40–43 the expression for the rate constants

$$k = A_{eff} \exp(-\Delta H/RT) \int_0^\infty P(E) \exp(-E/RT)\, dE \qquad (49)$$

For the case $\Delta H = 0$ and $l = 1$, at temperatures that are not too high, eq 49 is equivalent to the Bell[1] model of tunneling. A small difference arises because the permeability $G(E) = (1 + P(E)^{-1})^{-1}$ used by Bell for the case $l = 1$ and $P(E)$ used here differ in the region where $E \gtrsim E_d$. In this region the WKB approximation used in eq 40 and 41 is no longer valid and we set arbitrarily but not unreasonably

$$P(E \geq E_d) = 1 \qquad (50)$$

A_{eff} in eq 49 is an effective frequency factor given by

$$A_{eff} = (l/\pi^{l-1})\nu \exp(\Delta S/R) / \int_0^\infty \exp(-E/RT)\, dE = (l/(\pi^{l-1}RT))\nu \exp(\Delta S/R) \qquad (51)$$

A computer program was written in order to calculate the integrals in eq 49 numerically.

Discussion of the Kinetic Data in Terms of Tunneling. The calculated Arrhenius curves are shown together with the experimental rate constants in Figures 9 and 10. In principle, each set of Arrhenius curves is described by six experimentally independent parameters, there energies of activation, and three frequency factors. The good agreement between the experimental and the calculated curves shows, however, that using the tunneling model described above, each set of Arrhenius curves can be described by only four parameters. These are ΔH, log A, E_d, and Q', given in Table IV.

Table IV. Parameters Used for the Simulation of the Arrhenius Curves in Figures 8 and 9 according to the Tunneling Model Shown in Figure 7 As Compared to the Bell Model[a]

	model	ΔH/ (kJ mol^{-1})	log A_{eff}	Q'/Å	E_d/ (kJ mol^{-1})	$\Delta\epsilon$/ (kJ mol^{-1})
LL	Bell	24.3	10.8	0.082	35.6	0.0
LLL	Bell	27.2	11.2	0.05	37.7	0.0
LL	Figure 7	22.6	10.6	0.17	35.2	0.0
LLL	Figure 7	28.5	11.2	0.088	39.0	0.0

[a] ΔH, enthalpy of cyclic complex formation; n, number of transferred protons; A, frequency factor; E_d, barrier height; $\Delta\epsilon$, loss in zero-point energy at the top of the barrier. Q' is defined in eq 47.

Within this model the LLL reaction can be described by "chemically activated ground-state tunneling" as expressed by eq 37 and 41–43 and Figure 8a. The experimental energy of activation is then identified with the enthalpy of the cyclic complex formation. The model predicts that the RGM will be fulfilled within the margin of error as long as the different isotopic Arrhenius curves are nearly parallel.

For higher temperatures the model predicts a breakdown of the RGM. In the case of the LL reaction, for example, it predicts a value of k^{HD} which is smaller than the RGM value. By comparing Figures 9 and 10 it is apparent that this case is, in fact, under observation for the LL process. The deviation of k^{HD} from the RGM value is larger than the experimental error and is corroborated by the facts that the deviation is found over the whole temperature range and that it was detected by two independent methods. We obtained the rate constants of the HD reaction by ^{1}H NMR and by ^{2}H NMR (filled and open circles in Figure 9). In terms of the tunneling model, the LL transfer proceeds as indicated in Figure 8b in the cyclic complex from intermolecular excited states. In this tunneling regime the deviation of the HH/HD/DD KIE from the RGM parallels the asymmetry of $k^H/k^D/k^T$ KIE of single proton transfer in the presence of tunneling.[1] Since the LL and the LLL reactions proceed by tunneling, the Arrhenius curves do not contain information about the fifth parameter $\Delta\epsilon$ entering the above tunneling model, i.e., the difference in ZPE between the reactants and the proton-stable transition state of Figure 8c. We observed only significant changes of the other four parameters given in Table IV as long as $\Delta\epsilon$ was kept below a value of about 2–3 kJ mol^{-1}. We, therefore, preferred to set $\Delta\epsilon = 0$.

In view of the severe approximations used in the above tunneling model, we have to ask whether the parameters in Table IV have a physical significance. The values of ΔH for the LL and the LLL processes would seem to indicate that approximately 10 kJ mol^{-1} is lost per H bond when the cyclic complex (with nonlinear H bonds) is formed from the reactants (which form a linear H bond to the solvent). This result is very reasonable. Also reasonable are the values of the preexponential factors listed in Table IV. They contain the entropy of the cyclic complex formation, which is unknown. If one neglects this ΔS_0 in eq 38, one obtains for the true preexponential factor A_{ex} of the exchange reaction within the cyclic complex

$$\log A_{ex} = \log A_{eff} + n \log C_S \qquad (52)$$

With $C_S = 12.3$ M, we obtain log $A_{ex}^{LL} = 13$ and log $A_{ex}^{LLL} = 14$, which are both what is expected for an intramolecular reaction. The remaining two parameters in Table IV, E_d and Q', have to be discussed with more caution. Roughly, Q' is of the order expected from the dimensions of a H bond. Using eq 47, we obtain for the synchronous pathway a total proton transport distance $\Delta r = 0.68$ Å for the LL process and 0.35 Å for the LLL process. Assuming $l = 1$ (TR model) reduces these distances by a factor of 2. The same reduction is found when one assumes an asynchronous proton motion. The difference between the formation of an ion pair as intermediate shown in Scheme III and the

Scheme IV

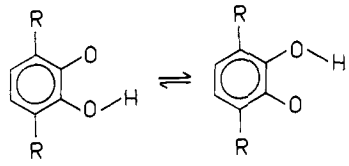

asynchronous tunneling pathway is that in the latter the total proton transport is complete before solvent molecules have reoriented in order to solvate the ion pair. The barrier E_d seems to be higher for the LLL process. The smaller value of Δr for the LLL process as compared to the LL process results in a faster exchange rate but a smaller KIE.

Behavior of KIE, similar to what we have seen, has been observed by other authors[61,62] for intramolecular proton transfer in 2-hydroxyphenoxyl radicals (HPR, Scheme IV), although no explanation was given by them. The bell criteria of tunneling, $A^H/A^D \ll 1$ and $E_a^D - E_a^H \gg 5$ kJ mol^{-1}, were fulfilled for a solution of the radical with R = *tert*-butyl in an inert solvent. However, upon the addition of the hydrogen-bond acceptor dioxane and with R = H the reaction rates were drastically reduced, the KIE increased, and A^D became less than A^H. This switch of the KIE is similar to the switch we observe between the LL and the LLL processes in the system acidic acid/methanol/THF. We were able[63] to simulate the Arrhenius curves of the process shown in Scheme III by using the tunneling model discussed here. We took into account that the radical must break an intermolecular hydrogen bond to dioxane before the proton transfer can take place. As a consequence, the arrangement of HPR seems to proceed along a soft double-minimum potential. This is in contrast to the TPP migration where the tightness of the potential results in sharp NH stretching bands[16] and a peculiar behavior seen for the HH/HD/DD KIE;[14] i.e., $k^{DD} = k^{HD} = k^{HH}/10$ at 298 K.

(61) Prokofiev, A. I.; Bubnov, N. N.; Solovnikov, S. P.; Kabachnik, M. I. *Tetrahedron Lett.* **1973**, 2479. Prokofiev, A. I.; Masalimov, A. S.; Bubnov, N. N.; Solodnikov, S. P.; Kabachnik, M. I. *Izv. Akad. Nauk SSSR, Ser. Khim.* **1978**, 310. Bubnov, N. N.; Solodnikov, S. P.; Prokofiev, A. I.; Kabachnik, M. I. *Russ. Chem. Rev. (Engl. Transl.)* **1978**, *47*, 1048.

(62) Loth, K.; Graf, F.; Andris, M.; Gunthardt, Hs. H. *Chem. Phys. Lett.* **1976**, *29*, 163. Loth, K.; Graf, F.; Gunthardt, Hs. H. *Chem. Phys.* **1976**, *13*, 95.

(63) Limbach, H. H.; Gerritzen D. *Faraday Discuss. Chem. Soc.* **1982**, *74*, 279.

Conclusions

By a new combination of dynamic ^{1}H and ^{2}H NMR spectroscopy we have succeeded in performing an NMR proton inventory of proton and deuteron exchange in the system acetic/acid/methanol/tetrahydrofuran. The rate constants k^{HH}, k^{HD}, k^{DD}, k^{HHH}, k^{HHD}, and k^{DDD} of cyclic double and triple proton transfer were determined as a function of temperature. This method of determining the number of protons transferred in the rate-limiting step, as well as the kinetic isotope effects, may be applied to a variety of chemically and biochemically important systems. The kinetic isotope effects themselves at 298 K can be explained by transition-state theory in terms of symmetric cyclic transition states. However, the dependence of the KIE on temperature did not follow the predictions of this theory. All the data can be accommodated with an intermolecular tunneling model which incorporates solvent effects. The single KIE are not very big, but the additional information inherent in the determination of the HH/HD/DD and HHH/HHD/DDD KIE provided evidence for tunneling. A very crude tunneling model presented here explains (with a minimum of four parameters) the complex behavior of the kinetic isotope effects as a function of temperature in several very different hydrogen-transfer reactions. From a theoretical viewpoint, the model is oversimplified. We are convinced that better models will be available in the future. The difficulty with models which are closer to reality is that they, generally, contain more adjustable parameters than can be extracted from the kinetic data. We hope that a systematic study of multiple kinetic isotope effects which have been very different for each reaction (which we have studied so far) will contribute to a better approach of theory and experiment.

Acknowledgment. We are indebted to Prof. R. P. Bell, R. L. Schowen, M. M. Kreevoy, and H. W. Zimmermann for helpful discussions of this work. We thank the Deutsche Forschungsgemeinschaft, Bonn, and the Fonds der Chemischen Industrie, Frankfurt, for financial support. The calculations were done on the Univac 1108 computer of the Rechenzentrum der Universität Freiburg.

Registry No. Acetic acid, 64-19-7; methanol, 67-56-1; deuterium, 7782-39-0; *meso*-tetraphenylporphine, 917-23-7.

Supplementary Material Available: Tables of inverse carboxylic proton lifetimes and inverse carboxylic deuteron lifetimes (6 pages). Ordering information is given on any current masthead page.